Analyst

COMMUNICATION

View Article Online
View Journal | View Issue

Cite this: *Analyst*, 2017, **142**, 3569

Received 15th March 2017,
Accepted 9th August 2017

DOI: 10.1039/c7an00454k

rsc.li/analyst

Controlled core-to-core photo-polymerisation – fabrication of an optical fibre-based pH sensor†‡

Fuad Mohamad, [a,b] Michael G. Tanner, [b,c] Debaditya Choudhury,[b,c] Tushar R. Choudhary,[b,d] Harry A. C. Wood,[e] Kerrianne Harrington[e] and Mark Bradley*[a,b]

The fabrication of fluorescence-based pH sensors, embedded into etched pits of an optical fibre *via* highly controllable and spatially selective photo-polymerisation is described and the sensors validated.

Optical sensors, utilising the many advantageous properties of visible light, have been developed to measure a variety of analytes, such as O_2, CO_2, pH, and glucose.[1–5] Optical fibres have been widely used in this area, driven by the increasing demand for small, compact, and simple robust sensors that can be delivered to a location remote from the optical measurement apparatus. Many optical fibre-based sensors have been constructed by immobilising indicators at the distal end of an optical fibre, where the indicators interact with the analytes, resulting in a measurable change in the optical properties.[3,6,7] This is often achieved by removing the cladding from the optical fibre which is replaced by a coating containing the specific indicator of choice.[8,9] In some cases, the tips of the fibres are chemically etched, and the indicator and/or a solid matrix is deposited into the etched cavities.[10,11]

Several fluorescence-based optical sensors have been fabricated using photo-initiation methods, employing the discrete optical pathways found in optical fibres.[12,13] The advantages of photo-induced polymerisation in controllable polymerisation are myriad, thus the polymer can be made *in situ* at room temperature, and patterned in defined locations.[7,14] Importantly, using an etched fibre means that the polymers generated are firmly anchored into the fibre, whereas placing indicators within a polymer matrix, and dip-coating onto the fibre tips, while widely reported,[13,15,16] can result in sensor leaching from the polymer matrices, poor attachment to the fibre itself, and photo-bleaching.[6,16]

Multicore optical fibres, due to their physical nature, offer a natural multiplexing potential. Walt has reported fibre-based photo-polymerisation by coupling light at the proximal end of an imaging fibre, thereby inducing photo-polymerisation of acryloyl fluorescein and 2-hydroxyethyl methacrylate, broadly on the illuminated area (Ø = 125 μm) at the distal end of the imaging fibre, thereby creating sensing regions for pH analysis.[7] This technique was expanded to the fabrication of a multi-analyte probe for pH, O_2, and CO_2, on a single imaging fibre (3000 individual elements), with discrete sensing areas (Ø = 27–47 μm).[14]

To date, no work has described the fabrication of an optical fibre-based sensor with discrete sensing cores within a multimode multi-core fibre. Herein, we report the fabrication of a novel, sensitive, and robust (physically and optically) fluorescence-based pH sensor by photo-polymerising fluorescein acrylate-based co-polymers at individually illuminated cores (with 405 nm illumination), which had been chemically etched to give pits by hydrofluoric acid (HF). The use of polymerisable fluorescent monomers overcomes the dye leaching problem,[17–21] and improves sensor photo-stability, while allowing photo-polymerisation directly into an etched core. This thereby secures the location of the sensor, resulting in enhanced fluorescence and robust attachment. The performance of the pH sensors was shown to be robust.

The general approach used for photo-polymerisation at the tip of the optical fibre is shown in Fig. 1. The optical fibres used in this work were multi-mode multi-core, consisting of 19 cores (diameter = 20 μm), made up from germanium-doped silica, and surrounded by a pure silica cladding. Each optical fibre was cut to 1 m length, with removal of a 5 cm length of coating at each side, followed by cleavage of each end (~1 cm) to give a smooth flat surface. One end of the optical fibres (distal end) was chemically etched in hydrofluoric acid (HF),

[a]*School of Chemistry, University of Edinburgh, Joseph Black Building, Edinburgh, EH9 3FJ, UK. E-mail: mark.bradley@ed.ac.uk*
[b]*EPSRC IRC Hub, MRC Centre for Inflammation Research, Queen's Medical Research Institute, University of Edinburgh, 47 Little France Crescent, Edinburgh, EH16 4TJ, UK*
[c]*Institute of Photonics and Quantum Sciences, Heriot-Watt University, Edinburgh, EH14 4AS, UK*
[d]*Institute of Biological Chemistry, Biophysics and Bioengineering, School of Engineering and Physical Sciences, Heriot-Watt University, Edinburgh, EH14 4AS, UK*
[e]*Department of Physics, University of Bath, Claverton Down, Bath, BA2 7AY, UK*
†Data used within this publication can be accessed at http://dx.doi.org/10.7488/ds/2118.
‡Electronic supplementary information (ESI) available. See DOI: 10.1039/c7an00454k

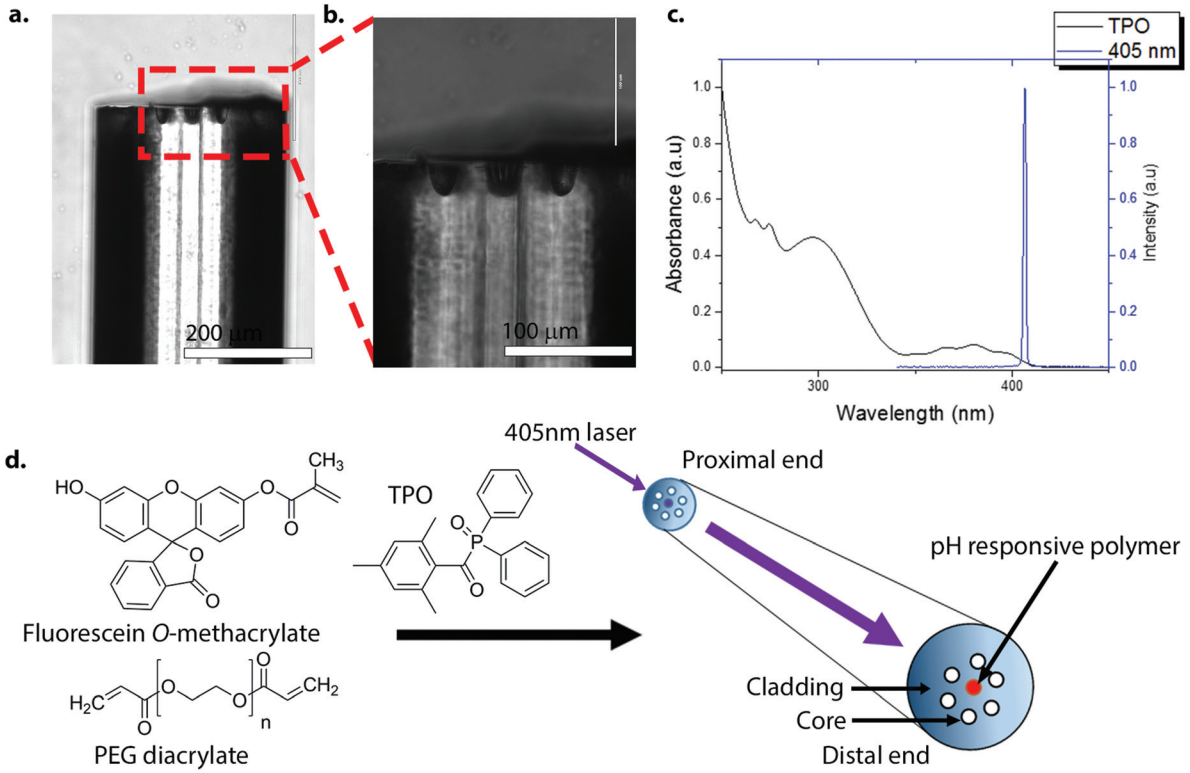

Fig. 1 (a)–(b) Lateral images of an etched optical fibre. The depth of a pit was approximately 30 μm. The distal end of the optical fibre was HF-etched and silanized in 3-(trimethoxysilyl)propyl methacrylate (TMSPMA) (20 v/v% in acetone) to introduce acrylate groups onto the distal surface of the pit. Scale bar (a) = 200 μm and scale bar (b) = 100 μm. (c) The absorbance spectrum of diphenyl(2,4,6-trimethylbenzoyl)phosphine oxide (TPO) (2.5 mM in ethanol) (black line), and the 405 nm laser spectrum (blue line). TPO absorbs in the UV range up to about 425 nm, and although not optimal, it allowed sufficient excitation and radical generation by TPO (it is worth noting that the light source used by dentists with this initiator are typically in the wavelength range of *circa* 380 to 520 nm (dual peak LED)).[23] (d) The method used for photo-polymerisation at the distal end of the optical fibre. Only seven (of the 19) cores of the optical fibre are shown for clarity. The laser was coupled to a specific core of the fibre *via* an XYZ translation stage. Once coupled, the distal end was dipped into the polymerisation solution containing fluorescein *O*-methacrylate 0.17 M, PEG-diacrylate 1.37 M and TPO 0.05 M.

which specifically removed the Ge-doped silica cores to form a cavity (or a pit) at the distal tip (Fig. 1a and b).[22] The etched fibres were then silanized with 3-(trimethoxysilyl)propyl methacrylate (TMSPMA) (20 v/v% in acetone), thereby introducing acrylate groups into the etched pits on the fibres. A 405 nm laser was used for photo-polymerisation as it was compatible with the absorbance spectrum of the photo-initiator, diphenyl(2,4,6-trimethylbenzoyl)phosphine oxide (TPO), a common dental photo-initiator that absorbs in the UV region up to about 425 nm (Fig. 1c).[23–25] To ensure uniform and controlled photo-polymerisation, the laser source was used at low power levels so that only a single core of the 19 cores was illuminated. Once coupled, the distal end of the fibre was placed into the polymerisation solution with the irradiation time and the laser power optimised for efficient photo-polymerisation. The polymerisation solution consisted of pH-sensitive fluorescein *O*-methacrylate 0.17 M, poly(ethylene glycol) diacrylate (PEGDa) 1.37 M as a cross-linker, and the photo-initiator TPO 0.05 M in *N*,*N*-dimethylacetamide (DMA). The transverse and lateral views of the optical set-up used for photo-polymerisation and fluorescence measurements are shown in Fig. S1.‡

Fig. 2 shows the transverse views of the optical fibres after photo-polymerisation with fluorescein *O*-methacrylate. Using too high a power and/or long irradiation times caused large bulbous polymers to form that extended beyond a single pit, covering, in extreme cases, the whole distal face of the fibre (Fig. S2‡). Using an illumination power of 100 μW and a 5 second illumination time, the polymerisation could be controlled, with polymer filling the etched pit of a single core (Fig. 2a and b). By coupling the laser to only one core at a time during the photo-polymerisation process, individual polymers could be grown at different cores, producing a sensor with multiple sensing elements. Fig. 2c shows the transverse view of an optical fibre containing three fluorescein *O*-methacrylate-based polymers.

A 485 nm laser was coupled to the "polymer cores" using a low excitation power (1.0 μW) to minimize the effects of photobleaching, with the photo-polymerised polymers showing a strong and robust pH dependent fluorescence, when pH > 6. The pH response of the sensor between pH 3 and pH 10 is shown in Fig. S3.‡ Sensor analysis between pH 6.6 and 7.6 was measured in 0.1 increments (in random order) with three calibration points (pH 6, 7, and 8) (Fig. 2d).§¶ Analysis of the

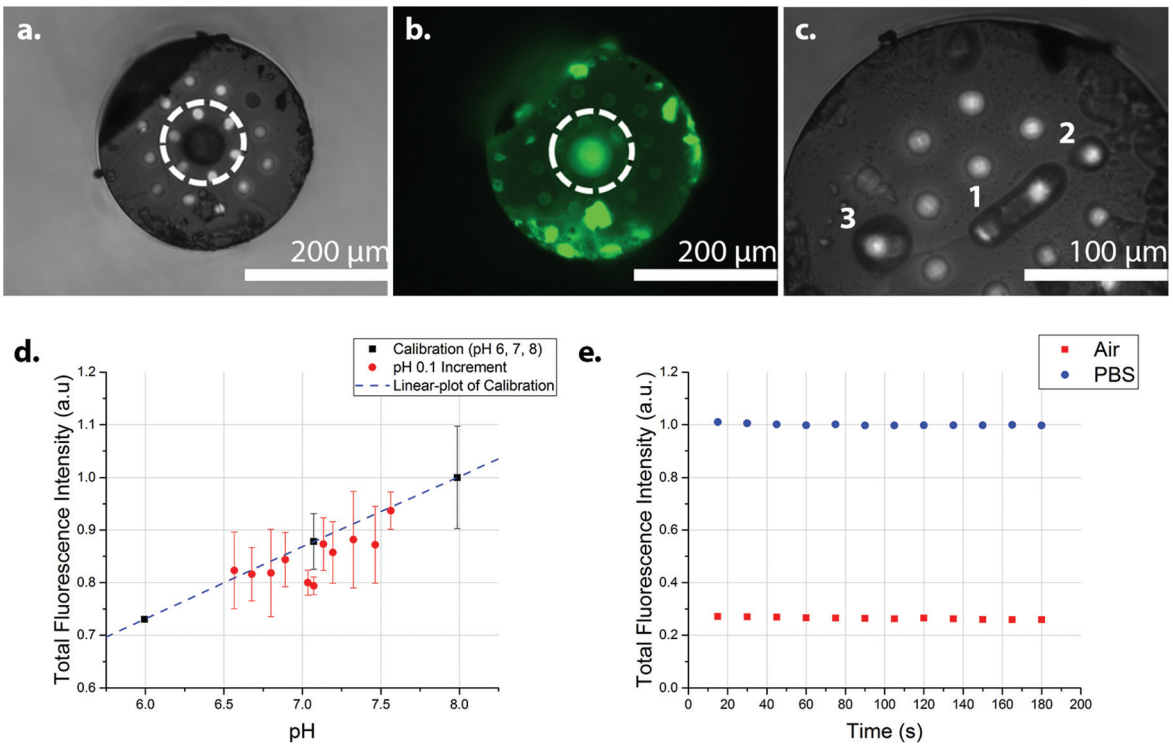

Fig. 2 Photo-polymerisation of fluorescein *O*-methacrylate and PEG diacrylate at the end of the optical fibre. (a) Image of the distal surface of an optical fibre, containing fluorescein polymer in the middle core (white circle) (b) The polymer fluoresced green under 470 nm excitation (white circle). (c) The distal surface of an optical fibre showing three fluorescein polymers (labelled 1, 2, and 3) at different cores. The polymers were grown individually, with defined core-to-core photo-polymerisation, with fresh polymerisation solution used for every polymerisation. The polymer labelled 1 distorted during photo-polymerisation thus extending to the next nearest core. The polymers generated filled the depth of the pits, thus giving polymer features of approximately 30 μm in depth (d) The integrated fluorescence intensity of the fluorescein *O*-methacrylate-based sensor at 0.1 pH increments from pH 6.6 to 7.6 (Fig. S4‡), with the three calibration points (pH 6, 7, and 8) (n = 2) (R^2 = 0.99). The fluorescence measurements of 0.1 pH increments were in random order, while the calibration points were in ascending order. (e) The integrated fluorescence intensity of the fluorescein polymer with continuous illumination for 180 seconds in PBS (pH 7.4) (blue circles) and in air (red squares), showing the photostability of the sensor. Very little evidence of photo-bleaching was observed. In a realistic use environment, discrete measurements would be performed, rather than the continuous illumination demonstrated here (180 seconds continuous exposure). The small variation of the intensity may also be attributed to the intensity fluctuations in the excitation source. All measurements were made in a dark room with an excitation wavelength of 485 nm, with the laser operating at 1.0 μW.

integrated fluorescence spectra showed little sign of photo-bleaching when the sensor was continuously illuminated in air or PBS for three minutes with the 485 nm laser operating at 1.0 μW (Fig. 2e). Randomised measurements in the range of 6.6 to 7.6 were generally within the error of the trend from the calibration data – although with some variations between the three replicates (Fig. S4‡), presumably from power variations in the laser. Analysis of the sensor response time (measured by measuring changes in the fluorescence intensity following the movement of the sensor from pH 6 to pH 8 and back to pH 6) gave a response time of 31 ± 3 seconds (Fig. S5‡).

In conclusion, an optical fibre-based pH sensor with discrete sensing cores was prepared. By combining photo-polymerisation and the discrete optical pathways of optical fibres, fluorescein-based polymers could be fabricated at individually irradiated cores. This allowed easy identification of the specific sensing cores for measurement and analysis, while the use of etched fibres allowed the fabrication of robust optical sensors. Furthermore, this technique allowed three polymers to be grown individually at three distinct cores, showing the potential of fabricating a multi-analyte sensor. Fluorescein *O*-methacrylate-based polymers at the irradiated cores showed robust pH dependence under physiological conditions with good repeatability. The use of an etched core enabled good attachment of the polymer, making the sensor package more robust in comparison with non-etched flat surfaced optical fibres, where there is a risk that polymer can detach from the distal end. Future work will focus on the development of a dual emission pH optical sensor to allow an internal reference to be added to the system to produce more reproducible optical pH sensors. This could be done by photo-polymerising the fluorescein monomer with other fluorescent monomers which acts as a reference dye.

Conflicts of interest

There are no conflicts to declare.

Acknowledgements

The work was supported by the Majlis Amanah Rakyat Mara (MARA) Malaysia (FM) and the UK Engineering and Physical Sciences Research Council (EPSRC, UK) Interdisciplinary Research Collaboration grant EP/K03197X/1.

Notes and references

§ The fluorescence set-up used a laser emitting at 485 nm (operating at 1.0 μW with a >510 nm band-pass filter). Measurements were performed by manually opening a shutter and recording the fluorescence spectrum with an integration time of 1 second. The manual shutter was closed between measurements to avoid any unnecessary photo-bleaching.

¶ pH 6–8 solutions were prepared using potassium dihydrogen phosphate (KH_2PO_4, 0.1 M), sodium hydroxide (NaOH, 0.1 M), and distilled water. The pH values were measured using a glass-electrode pH meter (Mettler Toledo), and where necessary adjustments were made using the appropriate acid or base.

1 C. McDonagh, C. S. Burke and B. D. MacCraith, *Chem. Rev.*, 2008, **108**, 400–422.
2 X. D. Wang and O. S. Wolfbeis, *Anal. Chem.*, 2016, **88**, 203–227.
3 M. C. Frost and M. E. Meyerhoff, *Annu. Rev. Anal. Chem.*, 2015, **8**, 171–192.
4 D. Wencel, T. Abel and C. McDonagh, *Anal. Chem.*, 2014, **86**, 15–29.
5 O. S. Wolfbeis, *BioEssays*, 2015, **37**, 921–928.
6 J. Lin, *Trends Anal. Chem.*, 2000, **19**, 541–552.
7 S. M. Barnard and D. R. Walt, *Nature*, 1991, **353**, 338–340.
8 M. Ahmad, K. P. Chang, T. A. King and L. L. Hench, *Sens. Actuators, A*, 2005, **119**, 84–89.
9 P. V. Preejith, C. S. Lim and T. F. Chia, *Meas. Sci. Technol.*, 2006, **17**, 3255–3260.
10 M. Bowden, L. Song and D. R. Walt, *Anal. Chem.*, 2005, **77**, 5583–5588.
11 S. Ahn, D. M. Kulis, D. L. Erdner, D. M. Anderson and D. R. Walt, *Appl. Environ. Microbiol.*, 2006, **72**, 5742–5749.
12 M. S. Purdey, J. G. Thompson, T. M. Monro, A. D. Abell and E. P. Schartner, *Sensors*, 2015, **15**, 31904–31913.
13 R. Song, A. Parus and S. Kopelman, *Anal. Chem.*, 1997, **69**, 863–867.
14 J. A. Ferguson, B. G. Healey, K. S. Bronk, S. M. Barnard and D. R. Walt, *Anal. Chim. Acta*, 1997, **340**, 123–131.
15 W. Jin, J. Jiang, X. Wang, X. Zhu, G. Wang, Y. Song and C. Bai, *Respir. Physiol. Neurobiol.*, 2011, **177**, 183–188.
16 E. J. Park, K. R. Reid, W. Tang, R. T. Kennedy and R. Kopelman, *J. Mater. Chem.*, 2005, **15**, 2913–2919.
17 L. Ferrari, L. Rovati, P. Fabbri and F. Pilati, *Sensors*, 2013, **13**, 484–499.
18 Y. Tian, B. R. Shumway, A. Cody Youngbull, Y. Li, A. K. Y. Jen, R. H. Johnson and D. R. Meldrum, *Sens. Actuators, B*, 2010, **147**, 714–722.
19 A. M. Breul, M. D. Hager and U. S. Schubert, *Chem. Soc. Rev.*, 2013, **42**, 5366–5407.
20 F. Thielbeer, S. V. Chankeshwara and M. Bradley, *Biomacromolecules*, 2011, **12**, 4386–4391.
21 H. R. Kermis, Y. Kostov and G. Rao, *Analyst*, 2003, **128**, 1181–1186.
22 K. R. Williams, K. Gupta and M. Wasilik, *J. Microelectromech. Syst.*, 2003, **12**, 761–778.
23 A. Santini, I. T. Gallegos and C. M. Felix, *Prim. Dent. J.*, 2013, **2**, 30–33.
24 L. F. J. Schneider, L. M. Cavalcante, S. A. Prahl, C. S. Pfeifer and J. L. Ferracane, *Dent. Mater.*, 2012, **28**, 392–397.
25 V. Miletic, P. Pongprueksa, J. De Munck, N. R. Brooks and B. Van Meerbeek, *J. Dent.*, 2013, **41**, 918–926.